Indian Journal of Chemistry
Vol. 61, May 2022, pp. 497-502

# Condensation product of 5-bromosalicylaldehyde and aminophenol: Fluorescence sensor for ascorbic acid and AND Logic Gate

Bidisha Bharali, Priyakshi Bordoloi & Diganta Kumar Das*

Department of Chemistry, Gauhati University, Guwahati, 781 014, Assam, India

*E-mail: diganta_chem@gauhati.ac.in

*Received 13 November 2021; revised and accepted 02 May 2022*

Condensation product (**L**) of 5-bromosalicylaldehyde and aminophenol has been synthesised and characterised. Fluorescence of **L** enhances by 23 times on interaction with $Ce^{3+}$ while it is quenched completely by $Ce^{4+}$. Ascorbic acid (AA) is a well known strong reducing agent and this property has been used to act **L**:$Ce^{4+}$ adduct as a fluorescence "on" sensor for AA. AA reduces $Ce^{4+}$ into $Ce^{3+}$ and thereby increasing fluorescence of **L** due to the formation of **L**:$Ce^{3+}$ adduct. Molecules which generally coexist with AA viz. Cholesterol, Glucose, Sucrose and Dopamine found not to interfere. The interaction of **L** with $Ce^{3+}$, $Ce^{4+}$ and subsequently with AA has been verified with cyclic voltammetry.

**Keywords**: Ascorbic acid, Cerium, Fluorescence, Logic Gate, Sensor, Voltammetry

Ascorbic acid (AA), commonly known as vitamin C, exists both in plants and animals. It has strong antioxidant property and takes part in a number of physiochemical and biochemical processes in human body. There is report that AA is associated with many chronic diseases like – gout, skin disease, infertility, mucositis, cancer and HIV/AIDS[1-3]. Due to strong antioxidant property AA can stop change in taste and smell in foods and beverages and therefore used in food, beverages, medical formula, cosmetics etc.[4]. AA is not synthesised in human body and need to be sufficiently supplemented through different food items in order to avoid many diseases. However excess intake of ascorbic acid may result in health problems such as urinary stones, diarrhoea, stomach cramps etc. Hence determination of AA in different food items is of great importance.

Because of its importance, AA has been determined by a number of different methods like – UV/visible spectroscopy[8,9], High Performance Liquid Chromatography (HPLC)[10], Electrochemistry[11-14] and Chemiluminescence[15]. But these methods are associated with drawbacks like –special sample preparation and high instrumentation cost. Fluorescence, as a technique, has advantages like - high sensitivity, simple sample preparation, relatively lower instrument cost, direct applicability to living cells and biological fluids[16-18].

There have been recent reports on fluorescence sensing of AA but most of them are based on nanoparticles and quantum dots (QD). Green emission fluorescent based on silicon nanoparticle (SiNP) and bovine serum albumin templated $MnO_2$ nanosheets is reported. Initially the fluorescence of SiNP is quenched by $MnO_2$ but AA on interaction reduces $MnO_2$ into $Mn^{2+}$ and SiNP gains back its fluorescence[19]. Fluorescent "on" sensor for the detection of AA has been developed based on the fluorescence resonance energy transfer (FRET) between graphene QDs and squaric acid (SQA)-$Fe^{3+}$[20]. $MnO_2$ nanosheets were interacted with $MoS_2$ QD to quench its fluorescence which is restored by interacting with AA due to reduction of $MnO_2$[21]. Self-assembly of 2,6-pyridine dicarboxylic acid sensitised $Eu^{3+}$ and carbon dots results resometric fluorescence response towards AA[22]. The blue fluorescence of SiNP was quenched by CoOOH nanoparticle and on interaction with AA the later nanoparticles are decomposed by redox process restoring the fluorescence of SiNP and hence facilitating sensing of AA[23]. In another method the fluorescence of CD is decreased by Ag NPs produced in situ by interaction of AA with Ag(I) in presence of Ag NP seeds[24]. Graphene QD was complexed with dopamine by electrostatic interaction and H-bonding which was then coordinated with $Cu^{2+}$ which quenched the fluorescence of QDs and the fluorescence quenching is removed by AA added to the solution resulting in AA sensing[25]. N doped CDs with high fluorescence

quantum yields have been reported which could detect AA by fluorescence "off" mode due to inner filter effect[26]. In another reported method, the fluorescence of N doped CD is quenched by Cr(VI) first, AA then reduces the Cr(VI) into Cr(III) restoring the fluorescence[27]. CdTe QDs have been reported to show red shift in fluorescence emission peak due to increase in its size on interaction with AA and hence acts as sensor for AA[28].

In this paper we report a very simple method for the detection of ascorbic acid where the fluorescence of the probe is first quenched by $Ce^{4+}$ and then AA reduced it into $Ce^{3+}$ leading to very large increase in fluorescence intensity. The method is found to be interference free from cholesterol, glucose, sucrose and dopamine. The probe acts as AND logic gate for fluorescence output with $Ce^{4+}$ and AA as input.

## Experimental Details

All the chemicals were either from Merck or Loba Chemie. The metal salts except $Pb(NO_3)_2$, $CaCl_2$ and $HgCl_2$ were sulphates. Metal salt solutions were prepared in doubly distilled water obtained from quartz double distillation plant. The FT-IR spectra were recorded in a Perkin Elmer RXI spectrometer as KBr pellets, $^1$H NMR and $^{13}$C NMR spectra were recorded on a Bruker Ultra Shield 300 MHz spectrophotometer using DMSO D6 as solvent. The fluorescence and UV/visible absorption spectra were recorded in HITACHI 2700 and Shimadzu UV 1800 spectrophotometer, respectively, using quartz cuvette (1 cm path length). Electrochemical experiments were performed at CHI (USA) electrochemical analyser work station 660D. Pt disc was used as working electrode, Ag-AgCl (3 N NaCl) as reference electrode and Pt wire as auxiliary electrode. Nitrogen gas was passed at slow rate through the solution to remove dissolved oxygen.

Condensation product (**L**) of 5-bromosalicyl-aldehyde and aminophenol was prepared by the method reported[29] earlier. The reaction is shown in Scheme 1. Briefly: an ethanolic solution of 1 mmol of 2-aminophenol (0.109 g) was added to the equimolar solution of 5-bromosalicylaldehyde (0.201 g) in absolute ethanol. The reaction mixture was stirred at room temperature for 7 h, yellow coloured precipitate was obtained, collected by filtration. UV-visible (1:1 *v/v* $CH_3OH$:$H_2O$, nm): 227, 422; FTIR (KBr, $cm^{-1}$): 3454 ($\nu_{OH}$),1624 ($\nu_{C=N}$), 762 ($\nu_{C-H}$); $^1$H NMR (DMSO D6, 300 MHz, ppm):13.890 (s, 2H,-OH), 10.2 (s, 1H, C-H), 8.925 (s, 1H, HC=N), 6.974-6.872 (m, 2H, J=9Hz), 7.157-7.108 (t, 2H), 6.546-6.357 (dd, 2H); $^{13}$C NMR (DMSO D6, 75 MHz, ppm)**:**206.99 (due to HC=N), 160.31, 160.18, 151.62, 135.43, 134.67, 134.16, 128.87, 121.61, 119.96, 119.69, 119.54, 116.87.

## Results and Discussion

**L** in 1:1 (*v/v*) $CH_3OH$:$H_2O$ ($5\times10^{-4}$ M) shows fluorescence spectrum on excitation with 270 nm photons in quartz cell of path length 1.0 cm. The emission was observed in 280 nm to 700 nm range with a maximum at 308 nm with intensity 360 (Fig. 1). Fig. 2 shows the fluorescence spectra of **L** in presence of one equivalent of different metal ions. From the figure it is clear that $Ce^{3+}$ enhances fluorescence of **L** significantly while $Ce^{4+}$ quenches the fluorescence of **L**. Metal ions - $Al^{3+}$, $Li^+$, $Na^+$, $Pb^{2+}$, $Cd^{2+}$, $Hg^{2+}$, $Mn^{2+}$, $Mg^{2+}$, $K^+$, $Ca^{2+}$, $Co^{2+}$, $Ni^{2+}$, $Cu^{2+}$ and $Zn^{2+}$do not effect fluorescence spectra of **L**. Fig. 3 shows the fluorescence spectrum of **L** in 1:1 (*v/v*) $CH_3OH$:$H_2O$ at different added concentration of

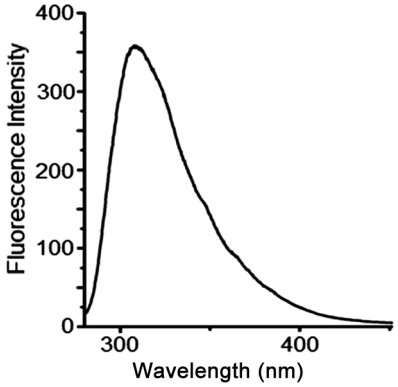


Fig. 1 — Fluorescence spectrum of **L** recorded in 1:1 $CH_3OH$:$H_2O$ (*v/v*). ($\lambda_{ex}$ 270nm, $\lambda_{max}$ 308 nm)

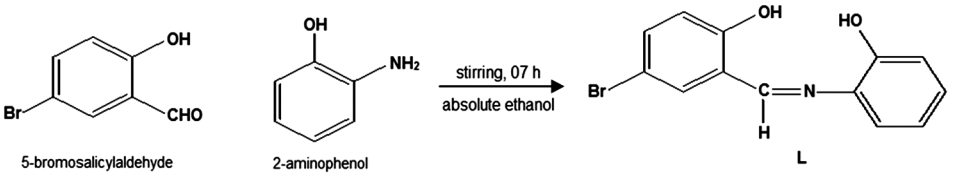


Scheme 1 — Synthesis of **L**

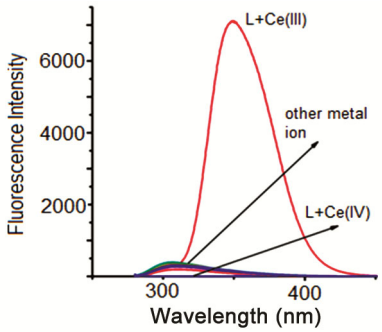


Fig. 2 — Fluorescence spectra of **L** in 1:1 (*v/v*) $CH_3OH$:$H_2O$ on addition of 100 µL of different metal solutions, $\lambda_{ex}$ 270 nm

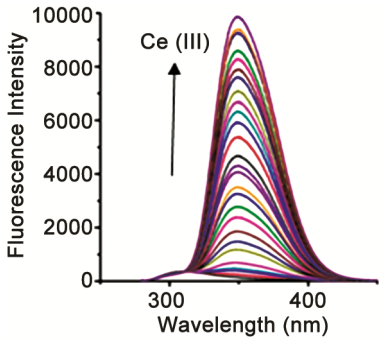


Fig. 3 — Fluorescence spectra of **L** in 1:1 $CH_3OH$:$H_2O$ (v/v) at different added concentration of $Ce^{3+}$, $\lambda_{ex}$ 270nm, $\lambda_{max}$ 348.6 nm

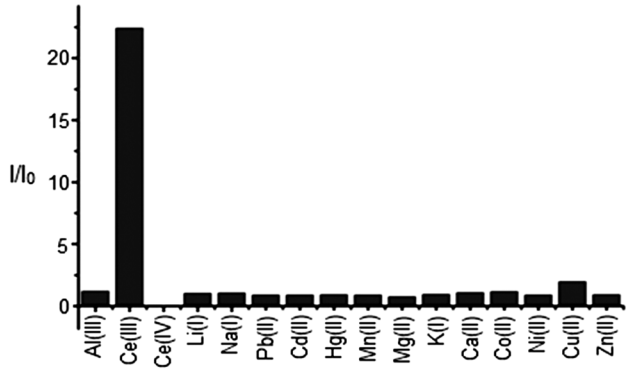


Fig. 4 — Bar diagram representing $I/I_0$ values for L in presence of different metal ions

$Ce^{3+}$. The $\lambda_{max}$ value for **L** was found to shift from 308 nm to 350 nm in presence of $Ce^{3+}$.

Fig. 4 shows the $I/I_0$ values where $I_0$ is the fluorescence intensity of **L** in absence of metal ions and I is the fluorescence intensity of **L** in presence of one equivalent of a particular metal ion in 1:1 (*v/v*) $CH_3OH$:$H_2O$. From the figure it is clear that $Ce^{3+}$ could enhance the fluorescence intensity of **L** by 22 times while in case of other metal ions it is below 2 times and $Ce^{4+}$ completely quenched the fluorescence intensity.

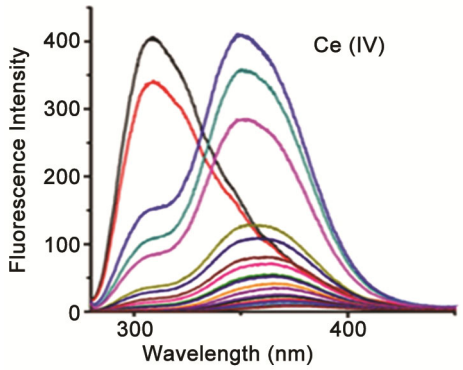


Fig. 5 — Fluorescence spectra of L in 1:1 (*v/v*) $CH_3OH$:$H_2O$ at different added concentration of $Ce^{4+}$, $\lambda_{ex}$ 270 nm

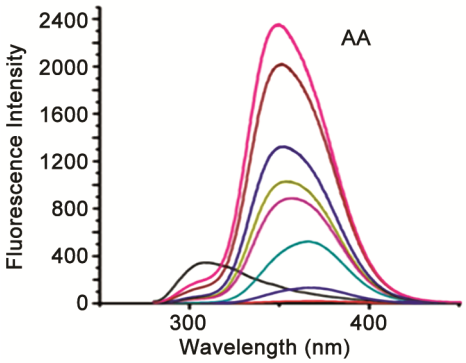


Fig. 6 — Fluorescence spectra of **L** with $Ce^{4+}$ in 1:1 (*v/v*) $CH_3OH$:$H_2O$ at different added concentration of ascorbic acid, $\lambda_{ex}$ 270 nm, $\lambda_{max}$ 350 nm

The fluorescence spectra of **L** in 1:1 (*v/v*) $CH_3OH$:$H_2O$) at different added concentrations of $Ce^{4+}$ is shown in Fig. 5. The 310 nm fluorescence peak initially shifts to 350 nm and then quenches with addition of $Ce^{4+}$ with $\lambda_{max}$ shifting towards 370 nm before complete quenching of fluorescence intensity. Fig. 6 shows the effect of fluorescence spectra of **L** in presence of one equivalent $Ce^{4+}$ and on subsequent addition of AA. It is observed that fluorescence intensity increases with red shift in $\lambda_{max}$ on addition of AA and finally the $\lambda_{max}$ becomes 350 nm which is same to that of **L** in presence of one equivalent $Ce^{3+}$. AA is a strong reducing agent and therefore it reduces $Ce^{4+}$ into $Ce^{3+}$ and the fluorescence enhancement is observed. Fig. 7 shows the plot of fluorescence intensity as a function of AA concentration which is linear.

The interference by molecules generally present in biological fluids closely with AA viz. Cholesterol, Glucose, Sucrose and Dopamine have been investigated. For the purpose fluorescence of **L**, **L** + $Ce^{4+}$, **L** + $Ce^{4+}$ + Interfering molecule + AA were

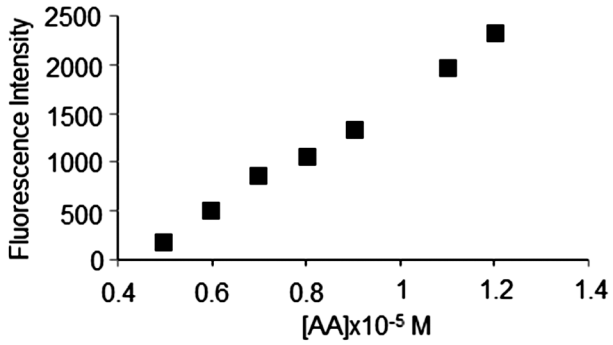


Fig. 7 — Fluorescence intensity of L:$Ce^{4+}$as a function of AA in 1:1 (*v/v*) $CH_3OH:H_2O$, $\lambda_{ex}$ 270 nm, $\lambda_{max}$ 350 nm

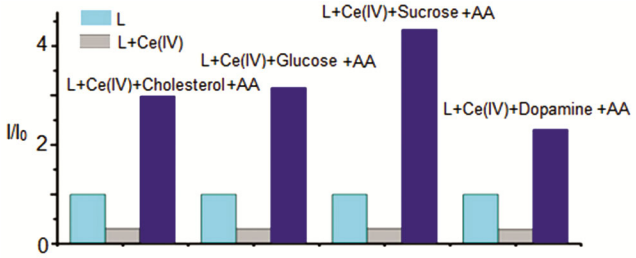


Fig. 8 — Plot of $I/I_0$ response of L (Green bars), L with Ce(IV) (Grey bars) and L, Ce(IV) + AA + other species (Blue bars) in 1:1 $CH_3OH:H_2O$ (*v/v*)

recorded. Here concentration ratios for all the species have been kept as one equivalent. Fig. 8 compares $I/I_0$ values through bars where $I_0$ is fluorescence intensity of **L** and I is the fluorescence intensity for **L** + $Ce^{4+}$ + Interfering molecule + AA. The comparable height of the bars, in presence of AA, and $I/I_0$ values similar to that for **L** + $Ce^{3+}$ (Fig. 8) confirms that Cholesterol, Glucose, Sucrose and Dopamine do not interfere detection of AA.

The effect of AA on **L** + $Ce^{4+}$ + AA has been examined by UV/visible absorption spectroscopy also. Fig. 9 shows the absorption spectrum of **L** + $Ce^{4+}$ in presence of different added concentration of AA in 1:1 (*v/v*) $CH_3OH:H_2O$. In absence of AA peaks were observed at 284 nm and 422 nm for **L** + $Ce^{4+}$ in 1:1 (*v/v*) $CH_3OH:H_2O$. On addition of AA the peak at 422 nm does not undergo any change while the absorbance of the peak at 284 nm increases gradually with a shift in $\lambda_{max}$ to 270 nm. Fig. 9, Inset shows the plot of absorbance versus AA concentration.

The interaction of **L** ($10^{-5}$ M) with $Ce^{4+}$ ($10^{-5}$ M) and **L** with $Ce^{4+}$ + AA ($1.5\times10^{-5}$ M) has been verified by cyclic voltammetry at Pt working electrode using Ag-AgCl (3 M NaCl) in 1:1 (*v/v*) $CH_3OH:H_2O$ (Fig. 10). The green curve is for **L**, the red curve is for **L**+$Ce^{4+}$ and the blue curve is for **L**+$Ce^{4+}$+AA. The

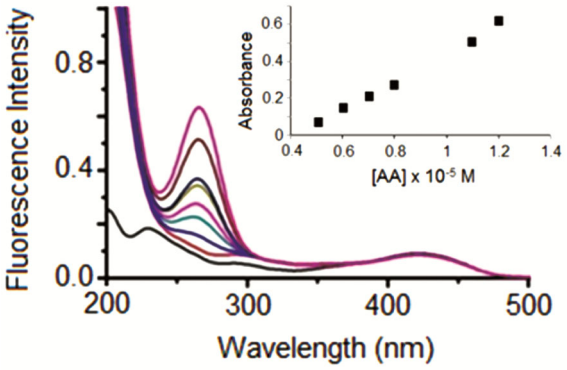


Fig. 9 — Change in the UV/visible absorption spectrum of L in 1:1 (*v/v*) $CH_3OH:H_2O$ in presence of $Ce^{4+}$ and different added concentration of Ascorbic acid

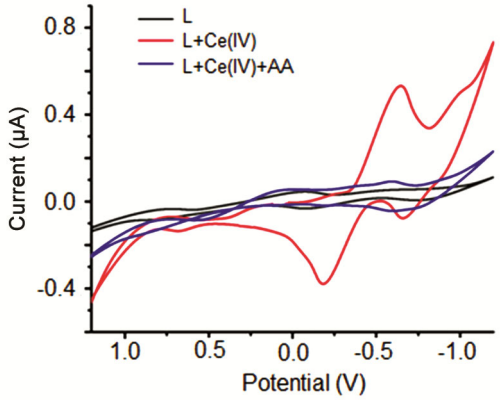


Fig. 10 — Cyclic voltammogram response of L in 1:1 (*v/v*) $CH_3OH:H_2O$ WE-Pt electrode, RE-Ag/AgCl, Scan rate 0.1 V/s

cyclic voltammograms for **L**+$Ce^{4+}$ is found to be quite different from that for **L**. Addition of AA leads to a cyclic voltammogram which is similar to that for **L**. This confirms that the interaction between $Ce^{4+}$ and **L** must be stronger than the interaction between $Ce^{3+}$ and **L**.

The fact that $Ce^{4+}$ quenches fluorescence of **L** while $Ce^{3+}$ enhances it can be explained (Scheme 2) considering the ionic radii of $Ce^{4+}$ and $Ce^{3+}$ which are 115 pm and 101 pm, respectively. Due to smaller size of $Ce^{4+}$ it can fit into the hole created by ONO of **L** and bind to the two O of hydroxyl groups and the immine N of **L**. Due to its higher charge to size ratio $Ce^{4+}$ withdraw the electron density from the conjugation system of **L** strongly and therefore the fluorescence is quenched. On the other hand, $Ce^{3+}$ being bigger do not fit into the hole and binds to the two O of the hydroxyls. Hence stops the PET process and fluorescence enhances. This also explains the different nature of cyclic voltammograms of **L** in presence of $Cr^{3+}$ and $Ce^{4+}$, since $Cr^{4+}$ affects the

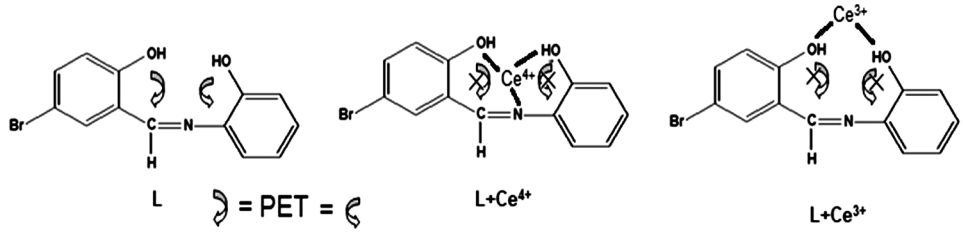


Scheme 2 — The PET involving lone electron pairs in hydroxyl groups in **L** causes low fluorescence of **L**; $Ce^{4+}$ quenches fluorescence of **L** by withdrawing electron density of **L** through immine N; $Ce^{3+}$ binds to hydroxyl O only and not to immine N due to bigger size thereby hinders PET process and enhances fluorescence of **L**

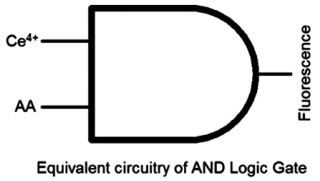


Scheme 3 — Schematic representation of AND Logic Gate

Table 1 — Truth table for AND Logic Gate

| INPUTS | | OUTPUTS |
|---|---|---|
| $Ce^{4+}$ | AA | AND |
| 0 | 0 | 0 |
| 1 | 0 | 0 |
| 0 | 1 | 0 |
| 1 | 1 | 1 |

conjugation system of **L**, its presence greatly influences the cyclic voltammogram of **L** while $Cr^{3+}$ does not affect the conjugation system of **L** and that is why the cyclic voltammogram is similar to that of **L**.

## AND Logic Gate

The response of $Ce^{4+}$ and AA towards **L** with respect to fluorescence forms the basis of AND Logic Gate truth table (Table 1, Scheme 3). Here the fluorescence generation has been assigned as 1 while no fluorescence enhancement has been assigned as 0.

## Conclusions

In conclusion, a new Schiff base fluorescence "off-on" sensor for ascorbic acid is reported. The sensor's fluorescence quenched by cerium(IV) ion is regenerated by ascorbic acid due to the reduction of cerium(IV) into cerium(III). The sensing of ascorbic acid is free of interference from Cholesterol, Glucose, Sucrose and Dopamine. The interaction between the sensor and cerium(IV) with ascorbic acid is confirmed by UV/Visible spectroscopy and cyclic voltammetry. The sensor with Cerium(IV) and ascorbic acid as inputs acts as AND logic gate.

## Acknowledgement

The authors thank DST, New Delhi for funding under MRP (EMR/ 2016/ 001745) and FIST to the department. PB thanks ASTEC, Guwahati for financial support.

## References

1 Drisko J A, Chapman J & Hunter V J, *J Am Coll Nutr*, 22 (2003) 118.
2 Choi H K, Gao X & Curhan G, *Arch Intern Med*, 169 (2009)502.
3 Pardakhty A, Ahmadzadeh S, Avazpour S & Gupta V K, *J Mol Liq,* 216 (2016) 387.
4 Xu Y-L, Niu X-Y, Chen H-L, Zhao S-G & Chen X-G, *Chin Chem Lett*, 28 (2017) 338.
5 Guo C, Jin Q, Wang Y, Ding B, Li Y, Huo J & Zhao X, *Sens Actuators B*, 234 (2016) 184.
6 Liu J, Chen Y, Wang W, Feng J, Liang M, Ma S & Chen X, *J Agric Food Chem*, 64 (2016) 371.
7 Li L, Wang C, Liu K, Wang Y, Liu K & Lin Y, *Anal Chem*, 87 (2015) 3404.
8 Sandulescu R, Mirel S & Oprean R, *J Pharm Biomed Anal*, 23 (2000) 77.
9 Llamas N E, Nezio M S D & Band B S F, *J Food Comp Anal*, 24 (2011) 127.
10 Szultka M, Buszewska-Forajta M, Kaliszan R & Buszewski B, *Electrophoresis*, 35 (2014) 585.
11 Liu B D, Luo L Q, Ding Y P. Si X, Wei Y, Ouyang X & Xu D, *Electrochim Acta*, 142 (2014) 336.
12 Tyszczuk-Rotko K, Beczkowska I, Wójciak-Kosior M & Sowa I, *Talanta*, 129 (2014) 384.
13 Chen L, Guo X M, Guo B, Cheng S K & Wang F, *J Electroanal Chem*, 760 (2016) 105.
14 Kingsley M P, Desai P B & Srivastava A K, *J Electroanal Chem*, 74 (2015) 171.
15 Dong Y P, Gao TT, Chu XF, Chen J & Wang CM, *J Luminsce*, 154 (2014) 350.
16 Sarma S, Devi B, Bhattacharyya P K & Das D K, *J Fluoresce*, 30 (2020) 1513.
17 Kumar J, Sarma M J, Phukan P & Das D K, *Dalton Trans*, 44 (2015) 4576.
18 Dutta K, Deka R C, Das D K, *J Luminsce,* 148 (2014) 325.
19 Xing K, Ge J, Wang W-X, Geng X, Shen X-P, Tang J-L, Qu L-B, Sun Y-Q & Li Z-H, *New J Chem*, 43 (2019) 9466.
20 Gao Y, Yan X, Li M, Gao H, Sun J, Zhu S, Han S, Jia L-N, Zhao X-E & Wang H, *Anal Methods*, 10 (2018) 611.

21 Xu Y-L, Niu X-Y, Chen H-L, Zhao S-G & Chen X-G, *Chin Chem Lett*, 28 (2017) 338.
22 Tian X & Fan Z, J Photochem Photobiol A, 413 (2021) 113261.
23 Lu Q, Chen X, Liu D, Wu C, Liu M, Li H, Zhang Y & Yao S, *Microchim Acta*, 186 (2019) 72.
24 Liu J, Wang L & Bao H, *Anal Bioanal Chem*, 411 (2019) 877.
25 Liu H, Li N, Zhang H, Zhang F & Su X, *Talanta*, 189 (2018) 190.
26 Kong W, Wu D, Li G, Chen X, Gong P, Sun Z, Chen G, Xia L, You J & Wu Y, *Talanta*, 165 (2017) 677.
27 Zhang Y, Fang X, Zhao H & Li Z, *Talanta*, 181 (2018) 318.
28 Zhu J, Zhao Z-J, Li J-J & Zhao J-W, *J Lumin*, 192 (2017) 47.
29 Patel K M, Patel K N, Patel N H, Patel M N, Chandrasekhar S & Cunico R F, *Synth React Inorg Met-Org Chem*, 30 (2008) 1965.